JOURNAL OF GUIDANCE, CONTROL, AND DYNAMICS
Vol. 30, No. 2, March–April 2007

Space Vehicle Conflict-Avoidance Analysis

Russell P. Patera*
The Aerospace Corporation, Los Angeles, California 90009-2957

DOI: 10.2514/1.24067

The concept of conflict probability, which is used in the aviation community, is proposed for use in space vehicle collision avoidance and collision risk reduction. Instead of a cylindrical conflict volume used by the aviation community, a spherical conflict volume is proposed for the space community. Mathematical techniques needed to implement the method are presented. Analysis of actual space collision events supports the use of conflict probability in identifying high-risk conjunctions. The dependence of conflict risk reduction on the maneuver threshold is found. The associated maneuver rate is also determined. Results are presented for various values of conflict volume radius. The method eliminates uncertainty caused by unreliable space object size data. Space object conflict probabilities are larger than associated collision probabilities and therefore are more easily interpreted.

Nomenclature

AR	=	aspect ratio, ratio of maximum to minimum standard deviation in the encounter plane
B	=	fraction of debris flux never resulting in a maneuver due to poor data quality
M_R	=	maneuver rate, number/year
m	=	maneuver threshold
P	=	conflict or collision probability
P_{Rf}	=	fractional reduction in probability rate due to maneuver threshold
P_{Rim}	=	conflict probability rate for the maneuver region, (number of conflicts)/year
P_{Rin}	=	net conflict probability rate, (number of conflicts)/year
Q_i	=	probability of a space vehicle being within the maneuver region for debris object approaching from the ith direction
R_i	=	radius of the maneuver keep-out region, m
r	=	distance from the primary object to the conflict area perimeter in the symmetrized encounter plane, m
ε_i	=	conflict area in encounter plane, m
η	=	residual conflict probability after a maneuver
θ	=	angular integration parameter
σ_i	=	standard deviation in the symmetrized encounter plane, m
Φ_i	=	flux of space debris objects approaching from the ith direction, number/m/year

Introduction

SPACE vehicle collision probability is replacing the closest approach distance as the parameter of choice for quantifying the collision risk. Methods to compute the probability of collision between two space objects were developed and presented in earlier publications [1–6]. The collision probability calculation involves the relative trajectory between the objects, the combined hardbody of the objects, and the combined relative position-error probability density. Mathematical techniques were developed to evaluate the collision probability for cases involving both linear and nonlinear relative motion between two space objects [7]. Recently, the nonlinear method was extended to larger hardbody sizes [8].

Although collision probability numbers can now be generated readily, the utility of the numbers is questionable, because the position uncertainty at the point of closest approach is too large and hardbody size data have a large amount of variability. As a result, the collision probability numbers are small, typically on the order of one in a million, as they were for the Cerise collision [9] that occurred in 1996. This low collision probability makes it more difficult to establish a maneuver criterion or threshold. As a result, many satellite operators use other parameters, such as the predicted closest approach distance, to supplement the collision probability when the maneuver decision is made.

Another difficulty with the collision probability value is that it depends upon the combined sizes of the space objects. An accurate size value may be available for an operator's own satellite, but only poor size information may be available for the secondary space object. A recent study found large variability in satellite size data based on radar cross section [10]. Thus, the collision probability value has a significant amount of uncertainty. The uncertainty and small value of the collision probability parameter limits its usefulness in the maneuver decision.

A remedy to the situation is proposed in this work. Instead of space vehicle collision probability, one should compute space vehicle conflict probability, similar to what the aviation community does regarding potential collisions between aircraft.

The aviation community uses a parameter referred to as conflict probability [11], which is very similar to space vehicle collision probability, except that the hardbody volume for conflict probability is defined to be a cylindrically shaped volume much larger that the actual sizes of the aircraft hardbodies. The cylindrical height of a conflict volume is aligned vertically. The circular cross section of the cylinder lies in the horizontal plane containing the north–south and east–west directions. The position-error covariances of the two aircraft are assumed Gaussian and are combined to form the relative position-error covariance matrix, which is centered on the primary aircraft. For aircraft free flight, the radius of the conflict volume is 5 n mile and its height is 4000 ft. The conflict volume is centered on the secondary aircraft. The probability that the primary aircraft will penetrate the conflict volume is the conflict probability. Because the conflict volume is very large compared with the actual aircraft sizes, the conflict probability can be larger than 0.1, which is orders of magnitude larger than space vehicle collision probability. In addition, use of the fixed conflict volume eliminates the need for hardbody size information. The large value of conflict probability is more easily interpreted and may help in establishing a meaningful conflict resolution maneuver threshold.

Conflict probability is proposed as a metric for identifying high-risk conjunction between space objects. Although the frequency of conflict resolutions in the space community is expected to be much

Presented as Paper 235 at the 16th AAS/AIAA Space Flight Mechanics Conference, Tampa, FL, 22–26 January 2006; received 20 March 2006; revision received 10 September 2006; accepted for publication 3 November 2006.

*Senior Engineering Specialist, Center for Orbital and Reentry Debris Studies, Mail Stop M4-066.

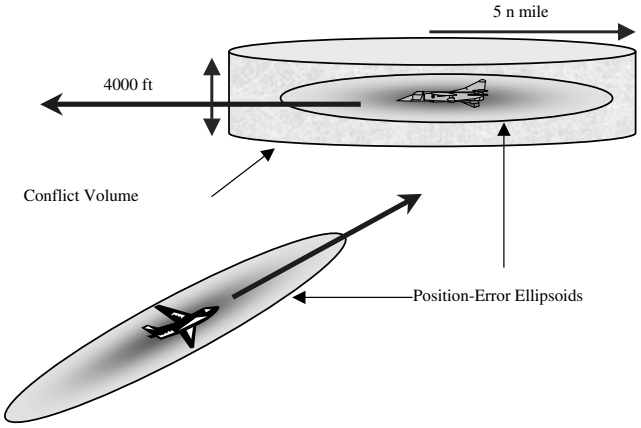

Fig. 1 Definition of conflict volume for an encounter between two aircraft.

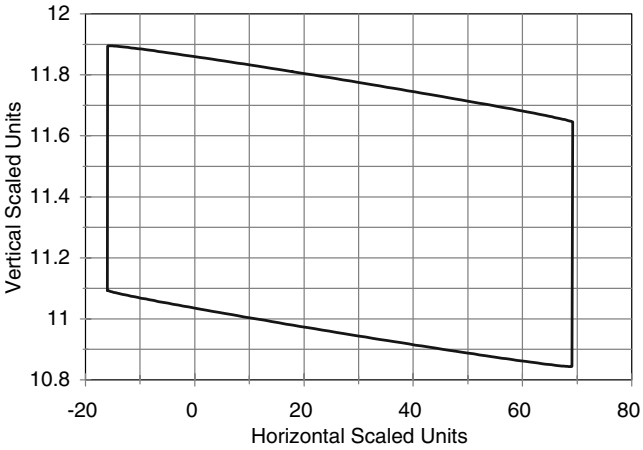

Fig. 2 Conflict area in the symmetrized encounter plane for the conflict volume used by the aviation industry.

less than that of the aviation community, the concept remains valid, because high-risk conjunctions need to be identified before further analysis determines which conjunctions require collision-avoidance maneuvers.

The space shuttle [12] and the International Space Station [13] use keep-out volumes that are centered on each vehicle to alert operators of a potential collision. If a debris object is predicted to penetrate the keep-out volume, a collision-avoidance maneuver is considered. This approach differs from the conflict probability method, which computes the probability that the conflict volume will be penetrated.

Spacecraft operators have used position-error probability density ellipsoids to identify potential collisions. If three-sigma ellipsoids of the respective space objects touch or intersect after the space objects are propagated to the point of closest approach, a potential collision is identified [14]. This approach differs from the conflict probability method, which computes the probability that a single conflict volume that is centered on one space object will be penetrated by the other space object.

Figure 1 illustrates aircraft conflict volume. One can use the aviation industry's conflict volume for space object encounters. Figure 2 illustrates the shape of the cylindrical conflict volume in the symmetrized encounter plane for the encounter associated with case 10 in Table 1. A cylindrical conflict volume is used for aircraft, because aircraft typically fly with constant altitude and encounters are mainly in the lateral direction.

Because space vehicles travel in elliptical orbits or circular orbits that change altitude according to orbital dynamics, a spherical conflict volume may be more appropriate. For spherical conflict volumes, conflict probability can be interpreted as the probability that the closest approach distance will be less than the conflict volume radius. This is a helpful interpretation when deciding if a conflict-avoidance maneuver should be performed. In addition, because spherical hardbody shapes are already in use for space vehicle collision probability, a spherical conflict volume would be easy to implement for space vehicles.

Once the size and shape of a conflict volume for space vehicles is established, conjunctions can be evaluated with consistency, because variations due to differences in hardbody sizes are eliminated. Using conflict probability, one has a uniform measuring stick to compare various conjunctions.

Conflict-avoidance maneuvers replace collision-avoidance maneuvers in reducing collision risk. Even for a single encounter, it may be difficult to decide if an avoidance maneuver is needed. Conflict-avoidance maneuver thresholds are helpful in determining when a maneuver should be executed. In addition, by executing conflict-avoidance maneuvers based on a conflict maneuver threshold, one reduces the long-term conflict probability.

Executing conflict-avoidance maneuvers does not completely eliminate the possibility of space vehicle confliction. However, the probability of conflict can be reduced to a desired level by selecting the appropriate maneuver threshold. This is analogous to what has been proposed for collision probability risk reduction [15,16]. Fortunately, methodology recently established for space vehicle collision risk reduction is applicable to the conflict risk reduction

Table 1 Comparison of conflict and collision probabilities

Case no.	Collision size, km	Collision probability	Rank	Conflict size, km	Conflict probability	Rank
1	1.035	9.55×10^{-5}	1	1	8.91×10^{-5}	13
2	0.203	9.31×10^{-5}	2	1	2.24×10^{-3}	1
3	1.035	9.05×10^{-5}	3	1	8.45×10^{-5}	15
4	0.107	2.01×10^{-5}	4	1	1.76×10^{-3}	3
5	0.100	1.79×10^{-5}	5	1	1.77×10^{-3}	2
6	0.096	9.67×10^{-6}	6	1	1.04×10^{-3}	6
7	0.202	3.21×10^{-6}	7	1	7.86×10^{-5}	16
8	0.136	2.04×10^{-6}	8	1	1.11×10^{-4}	11
9	0.036	1.73×10^{-6}	9	1	1.37×10^{-3}	4
10	0.035	1.33×10^{-6}	10	1	1.08×10^{-3}	5
11	0.093	5.22×10^{-7}	11	1	6.03×10^{-5}	19
12	0.058	3.09×10^{-7}	12	1	9.14×10^{-5}	12
13	0.036	1.91×10^{-7}	13	1	1.49×10^{-4}	7
14	0.035	1.74×10^{-7}	14	1	1.38×10^{-4}	9
15	0.035	1.72×10^{-7}	15	1	1.40×10^{-4}	8
16	0.035	1.57×10^{-7}	16	1	1.27×10^{-4}	10
17	0.035	1.11×10^{-7}	17	1	8.86×10^{-5}	14
18	0.035	9.80×10^{-8}	18	1	1.82×10^{-5}	17
19	0.036	9.36×10^{-8}	19	1	7.30×10^{-5}	18
20	0.035	5.33×10^{-8}	20	1	4.33×10^{-5}	20

problem [17]. Hardbody size is replaced with conflict volume in the analysis. Spherical conflict volumes of several different sizes are used to compute conflict risk reduction and the associated maneuver rate for a set of space vehicle conjunctions. In this paper, conflict probability is compared with collision probability for a set of space object conjunctions. The maneuver rate and conflict risk are found for various values of the conflict maneuver threshold. The usefulness of conflict probability in identifying high-risk conjunctions is established using conjunction statistics associated with three known space collision events.

Comparison of Collision Probability and Conflict Probability

Collision probability is the integral of the relative position-error probability density over the volume swept out by the combined hardbody as the space objects pass one another. For linear relative motion, the three-dimensional integral was reduced to a one-dimensional contour integral about the projection of the combined hardbody in the encounter plane, as presented in Eq. (1), in which P is the collision probability, r is the distance from the primary object to the hardbody perimeter (centered on the secondary object), and σ is the symmetrized position-error standard deviation. Symmetrization is required to reduce the probability calculation to that of evaluating a one-dimensional contour integral. Finding the principal axes of the position-error ellipsoid and performing scale changes along two of the principal axes achieves symmetrization. The magnitude of each scale change is selected to make its associated position-error standard deviation equal to that of the third principal axis. The position-error ellipsoid becomes spherical in the symmetrized frame. The scale changes needed for the symmetrization are applied to state vectors and points defining the combined hardbody boundary. Details of the derivation of the probability integral can be found in the original paper [4] and in a more general work involving nonlinear relative motion cases [8].

$$P = \frac{1}{2\pi} \oint_{\text{perimeter}} \left[1 - \exp\left(\frac{-r^2}{2\sigma^2} \right) \right] \mathrm{d}\theta \tag{1}$$

The collision probabilities for a set of 20 encounters are presented in Table 1, along with the combined hardbody sizes (collision size). In addition, the values of the collision probabilities were ranked according to risk.

Conflict probability is computed using Eq. (1), but with the perimeter defined as the perimeter of the conflict area in the encounter plane, rather than in the hardbody area. Conflict probability can be interpreted as the probability that the primary object will penetrate the conflict volume that is centered on the secondary object during the encounter. For a spherical conflict volume, this is equivalent to the probability that the objects will approach each other to a range less than the radius of the conflict volume.

Conflict probabilities were computed for each case in Table 1, assuming a spherical conflict volume with a radius of 1 km. A computer simulation valid for both linear and nonlinear relative motion [8] was used to ensure the validity of the probabilities in the event of a nonlinear relative motion encounter. Conflict probability results, along with relative ranking according to risk, appear in Table 1 for comparison purposes. Results in Table 1 indicate that the conflict probabilities are much greater than the collision probabilities, as expected. In addition, the ranking according to conflict risk differs from that of collision risk. Figure 3 illustrates the magnitudes of conflict probability and collision probability for the 20 cases in Table 1.

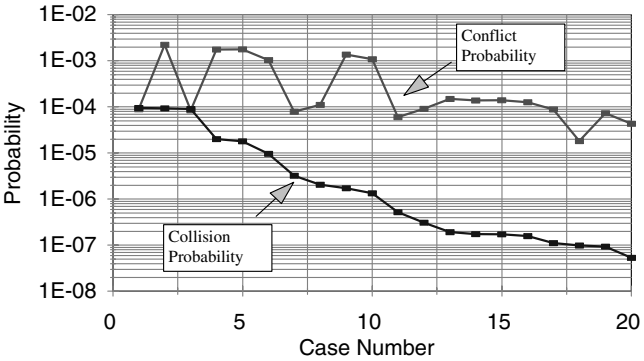

Fig. 3 Comparison of conflict and collision probability for cases in Table 1.

The advantage that conflict probability has over collision probability can be illustrated by revisiting the Cerise collision that occurred 24 July 1996. Using state vector data for object numbers 23606 (Cerise) and 18208 (debris), a close approach of 1–2 km was estimated [9]. Covariance and combined hardbody size information was not available at the time of initial analysis [9]. Assuming a symmetrical position-error standard deviation of 1 km and a hardbody radius of 5 m, one finds a collision probability of 4.23×10^{-6}, which is roughly consistent with published results [9]. It is unclear, based on this very low collision probability, that a maneuver is warranted. Because a collision did occur, one needs an improved collision prediction method. Conflict probability could serve this purpose. If a conflict volume having a radius of 1 km is used, the conflict probability is 0.169. Conflict probability is reduced to 0.0425 if the conflict volume radius is reduced to 500 m. Conflict probability is the probability that the debris object will penetrate the spherical conflict volume that is centered on Cerise. A conflict probability of 0.169 or 0.0425 is sufficiently large to indicate that a conflict-avoidance maneuver may be needed. In addition, object size data are not required for conflict probability prediction. A large value of conflict probability indicates a high-risk conjunction, but does not always result in executing a maneuver. Further analysis of high-risk conjunctions using higher accuracy data should be performed before a maneuver decision is made.

Conflict Probability and Collision Risk

Conflict probability is one indicator of collision risk. Other indicators are closest approach distance and collision probability. Statistical analyses of three known collision events [18] were used to access how well conflict probability predicts collision risk. The 23 December 1991 collision between object numbers 13475 and 18985, the 24 July 1996 collision between object numbers 18208 and 23606, and the 17 January 2005 collision between object numbers 7219 and 26207 were investigated. Each collision event involved objects from unrelated launches, and so no "parent–child" effects exist that would tend to increase collision probability. In fact, the debris object that collided with Cerise in 1996 was launched in 1986, but Cerise itself was launched in 1995. The entire unclassified catalogue of tracked objects was screened for conjunctions of less that 5 km over a five-day period, centered at the time of each collision. Databases of space object sizes and estimated covariances were used in the calculations. Table 2 contains the collision and

Table 2 Conflict and collision probabilities for space collision events

Collision year	Collision probability	Maximum conjunction probability	Conflict probability $R = 500$	Conflict probability $R = 750$	Conflict probability $R = 1000$
1996	2.89e-7	1.95e-6	0.045	0.145	0.3118
2005	7.86e-7	1.20e-4	0.2096	0.3545	0.479
1991	1.05e-5	1.28e-5	0.218	0.3942	0.556

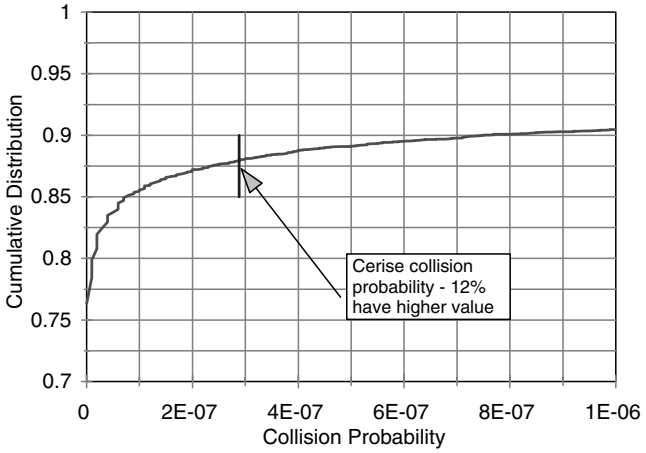

Fig. 4 Cumulative distribution of collision probabilities associated with the 1996 Cerise collision event.

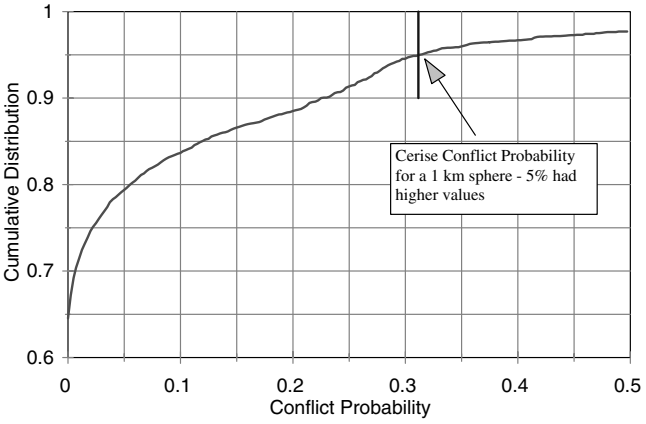

Fig. 5 Cumulative distribution of conflict probabilities associated with the 1996 Cerise collision event.

conflict probabilities for the three collision events. The collision probability for the 1996 Cerise collision event differs from the earlier rough estimate, due to hardbody size and position-error covariance differences. Table 2 also includes results from the recently proposed "maximum conjunction probability" [19]. This method adjusts position uncertainty to maximize collision probability but does not change the miss distance. Figure 4 illustrates collision probability results for the 1996 collision event. Twelve percent of the 8718 conjunctions had greater collision probability than the objects that actually collided. Figure 5 illustrates results for conflict probability. Five percent of the 8718 conjunctions had greater conflict probability using a 1-km conflict volume radius. Table 3 and Fig. 6 summarize the results for all three collision events. Numbers shown are the percentages of conjunctions having higher values of the given parameter. A smaller percentage is preferable, because there would be fewer "false alarms." Conflict volume radii of 500, 750, and 1000 m were included for comparison purposes. Table 3 also includes results for maximum conjunction probability. For the 1996 collision event, 21.7% of the 8718 conjunctions had higher maximum conjunction probability than the collision event itself. These results indicate that the maximum conjunction probability

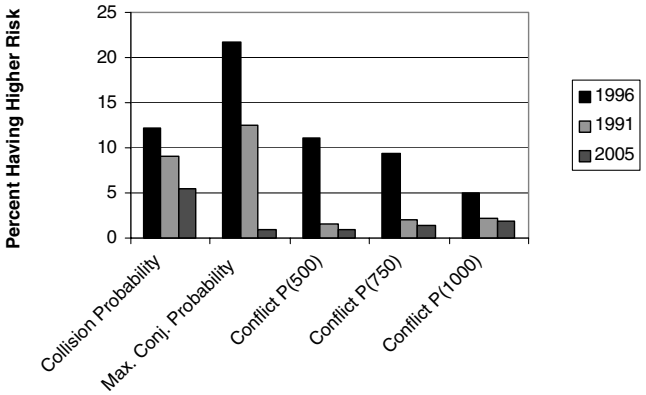

Fig. 6 Conjunction statistics for three space collision events.

parameter is not a very good indicator of collision risk and is not recommended for identifying high-risk conjunctions. The results clearly indicate that conflict probability is a better indicator of collision risk than collision probability or maximum conjunction probability. Further analysis should be performed to determine the optimum conflict volume size and shape.

Conflict Risk Reduction

A conflict-avoidance maneuver may be executed if the conflict probability exceeds a conflict-avoidance threshold. If a conflict-avoidance maneuver is performed every time the conflict probability exceeds the threshold, the long-term conflict probability is reduced. The lower the conflict-avoidance threshold, the greater the maneuver rate and the lower the long-term conflict risk. Relationships among long-term collision risk, collision-avoidance maneuver threshold, and collision-avoidance maneuver rate were previously developed [17]. The same methodology can be used for long-term conflict probability reduction. For conflict probability reduction, the hardbody volume is replaced with the much larger conflict volume.

Although debris objects can approach a space vehicle from any direction, we first solve the problem for a single encounter direction. The full problem is solved by combining results from all encounter directions. Alternatively, one can choose a single encounter direction with parameters that are representative of the full problem. Assuming that debris objects are incident from a small solid angle that is centered along the *i*th direction, the conflict probability rate can be computed for any desired region in the associated encounter plane. The conflict probability rate associated with the conflict maneuver region shown in Fig. 7 is given by

$$P_{Rim} = \varepsilon_i \Phi_i \left[1 - \frac{1}{2\pi} \oint_{\text{conflict maneuver region}} \exp\left(\frac{-R_i^2}{2\sigma_i^2} \right) \mathrm{d}\theta \right] = \varepsilon_i \Phi_i Q_i \tag{2}$$

where

$$Q_i = 1 - \frac{1}{2\pi} \oint_{\text{conflict maneuver region}} \exp\left(\frac{-R_i^2}{2\sigma_i^2} \right) \mathrm{d}\theta \tag{3}$$

and σ_i is the symmetrized position-error standard deviation. Q_i can be interpreted as the probability of the space vehicle being within the conflict maneuver region, which is bounded by the contour $R_i(\theta)$. The conflict probability rate can be reduced by performing a conflict-avoidance maneuver each time an individual probability is greater

Table 3 Conjunction statistics for collision and conflict probabilities

	Number of conjunctions	Percent higher collision probability	Percent higher conflict probability $r = 500$ m	Percent higher conflict probability $r = 750$ m	Percent higher conflict probability $r = 1000$ m	Percent higher maximum conjunction probability
1996	8718	12.12	11.14	9.2	5.03	21.7
2005	1042	5.53	1.0	1.37	1.9	1.0
1991	7525	9.00	1.5	2.00	2.18	12.5

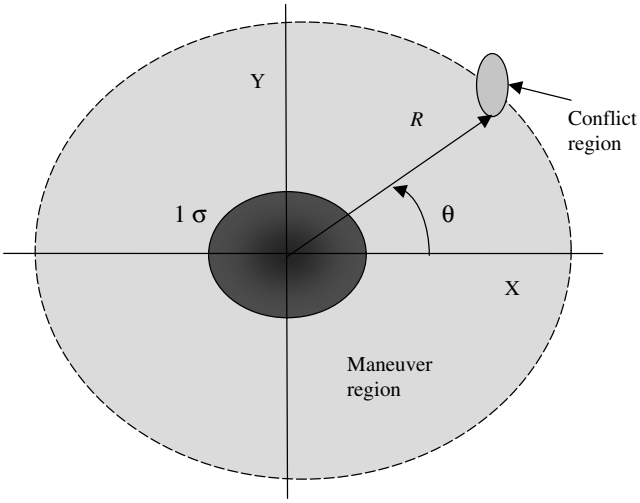

Fig. 7 Encounter plane after symmetrization.

than a maneuver threshold. This occurs when the space vehicle is within the maneuver region.

If the space vehicle is maneuvered each time it is within the maneuver region and its resulting conflict probability is zero after the maneuver, the net conflict risk is found by subtracting Eq. (2) from the conflict probability rate for the entire encounter plane $\varepsilon_i\Phi_i$.

$$P_{\text{Rin}} = \varepsilon_i\Phi_i - \varepsilon_i\Phi_i Q_i = \varepsilon_i\Phi_i(1 - Q_i) \tag{4}$$

Once a vehicle is maneuvered, its conflict probability is not necessarily zero. It may have a residual conflict probability given by η. In this case, the net conflict probability increases by $\varepsilon_i\Phi_i Q_i\eta$ and is given by

$$P_{Rin} = \varepsilon_i\Phi_i - \varepsilon_i\Phi_i Q_i + \varepsilon_i\Phi_i Q_i\eta = \varepsilon_i\Phi_i[1 - (1 - \eta)Q_i] \tag{5}$$

There are situations in which maneuvers are not advisable, because the position-error standard deviation is too large. For example, the direction in which to maneuver may not be clear. In these cases, we have a fraction B of the flux of objects that cannot result in conflict-avoidance maneuvers, and so Q becomes $Q(1 - B)$ and Eq. (5) becomes

$$P_{Rin} = \varepsilon_i\Phi_i[1 - (1 - \eta)(1 - B)Q_i] \tag{6}$$

If the maneuver region is zero ($Q_i = 0$), there are no maneuvers and $P_{Rin} = \varepsilon_i\Phi_i$, as expected. If the maneuver region is very large, $Q_i = 1$ and $P_{Rin} \approx \varepsilon_i\Phi_i(B + \eta - B\eta)$. However, one should not maneuver if the probability is less than η.

Because debris objects can approach from all directions, one can compute average representative encounter-plane parameters, which appear without the subscript i. Therefore, the i subscript will be dropped. The fractional reduction in conflict risk can be computed by dividing Eq. (6) by $\varepsilon\Phi$.

$$P_{Rf} = 1 - (1 - \eta)(1 - B)Q \tag{7}$$

The maneuver rate is the flux minus the background flux times the area of the maneuver region bounded by R.

$$\begin{aligned} M_R &= \frac{\Phi(1 - B)}{AR} \oint_{\text{conflict maneuver region}} \int_0^{R(\theta)} r\,\mathrm{d}r\,\mathrm{d}\theta \\ &= \frac{\Phi(1 - B)}{2(AR)} \oint_{\text{conflict maneuver region}} R^2\,\mathrm{d}\theta \end{aligned} \tag{8}$$

AR is the ratio of maximum to minimum position-error standard deviation in the encounter plane before symmetrization. Symmetrization reduces the flux by the factor $1/AR$, due to the associated scale change. In general, R is a function of θ in Eq. (8). Equations (7) and (8) are valid for arbitrary conflict volume size. If the conflict volume size is much less than the position-error standard deviation, the maneuver region becomes circular in shape and R takes a constant value. In this case, Q and M_R become, respectively,

$$Q = 1 - \exp\left(\frac{-R^2}{2\sigma^2}\right) \tag{9}$$

$$M_R = \frac{\Phi(1 - B)\pi R^2}{AR} \tag{10}$$

The maneuver threshold m is equal to the conflict probability at the maneuver boundary, which is equal to the conflict area $AR\varepsilon$ times the position-error probability density at the maneuver boundary. Therefore, the maneuver threshold is given by

$$m = \frac{AR\varepsilon}{2\pi\sigma^2}\exp\left(\frac{-R^2}{2\sigma^2}\right) \tag{11}$$

Using Eq. (11), the parameter R in Eq. (9) can be replaced by the maneuver threshold m. The result reduces Eq. (7) to Eq. (12) after some algebraic manipulation.

$$P_{\text{Rf}} = (B + \eta - B\eta)\left(1 - \frac{2\pi m\sigma^2}{(AR)\varepsilon}\right) + \frac{2\pi m\sigma^2}{(AR)\varepsilon} \tag{12}$$

Equation (11) is used to reduce Eq. (10) to Eq. (13) after algebraic manipulation.

$$M_R = \frac{(1 - B)2\pi\Phi\sigma^2}{AR}\{\ell_n[(AR)\varepsilon] - 2\,\ell_n(\sigma) - \ell_n(m) - \ell_n(2\pi)\} \tag{13}$$

Equation (13) contains the dependence of the maneuver rate on the hardbody area, position uncertainty, and maneuver threshold. Equations (12) and (13) are valid only when the conflict volume size is much less than σ. Therefore, they should be used for collision risk reduction, but not conflict risk reduction.

Numerical Results

A computer program was developed to implement the conflict probability reduction method. The first task was to compute the maneuver region boundary. This was achieved by fixing the direction of r in the encounter plane and varying its magnitude until the desired threshold was reached. A scale change was performed to symmetrize the position-error uncertainty. The maneuver region in the symmetrized encounter plane is usually not circular in shape. Once the maneuver region is defined in the symmetrized encounter frame, the associated maneuver rate and conflict probability reduction could be computed.

Figure 8 illustrates the maneuver region in the symmetrized encounter plane for threshold $= 0.1$, $AR = 2$, $\Phi = 2.7\times$

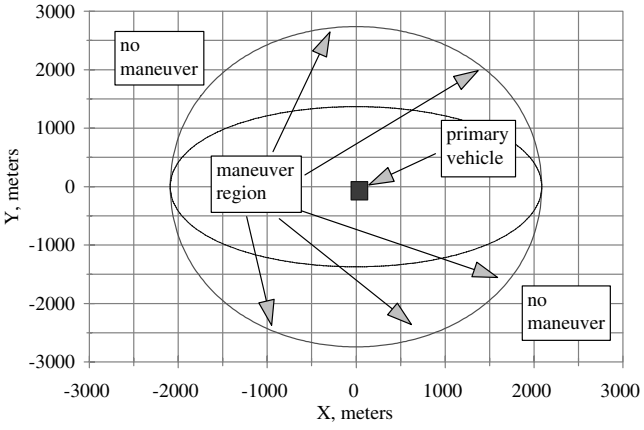

Fig. 8 Conflict probability maneuver region in the symmetrized encounter plane.

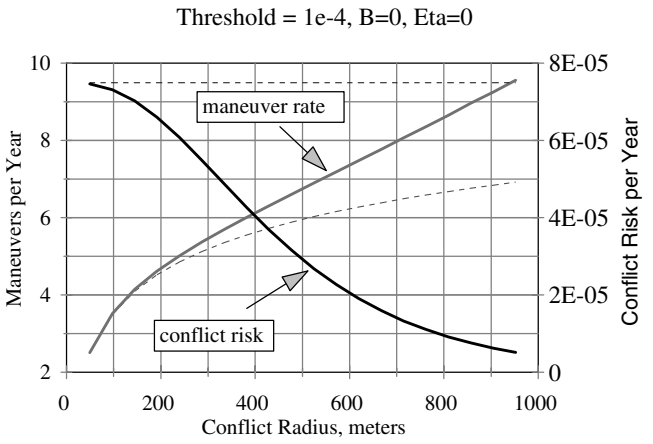

Fig. 9 Collision risk and maneuver rate versus conflict volume radius.

10^{-7} no./m^2/yr, $r = 1000$ m, $\sigma = 940$ m, $\eta = 0$, and $B = 0$. Also shown is the maneuver region before symmetrization, indicated by the inner contour. The maximum axis was aligned with the x axis, for convenience. The debris flux was integrated over the maneuver region using Eq. (8) to obtain the maneuver rate of 2.45 maneuvers per year. Equation (3) was used to obtain Q, which was used in Eq. (6) to obtain the reduced annual conflict probability of 0.0386. This means that a debris object will penetrate the 1-km conflict sphere 386 times in 10,000 years. If no maneuvers were performed, the annual conflict probability would be 0.848, meaning that a debris object would penetrate the conflict sphere 8,480 times in 10,000 years.

Figure 9 illustrates conflict risk and maneuver rate for various values of the radius of the conflict sphere. Both B and η are zero, $\phi = 2.7 \times 10^{-7}$ no./m^2/yr, $\sigma = 940$ m, and the maneuver threshold is 1×10^{-4}.

The heavier curves in Fig. 9 represent the correct values obtained from explicitly computing the maneuver region, whereas the dashed curves represent results using Eqs. (6), (12), and (13), which are applicable for smaller conflict volume size. Notice that the results are in agreement when the conflict radius is 50 m or less. Because the threshold was fixed, a larger conflict volume radius increases the maneuver region and associated maneuver rate. The associated conflict risk decreases dramatically. The erroneous dashed curve showing constant conflict risk is included in Fig. 9 for illustrative purposes only.

Figure 10 illustrates results for the same case as in Fig. 9, but with $\eta = 1 \times 10^{-4}$. The conflict risk decreases, then increases, for increasing conflict radius.

Figure 11 illustrates results for the same case as in Fig. 9, but with $\eta = 1 \times 10^{-5}$, which is much less than the threshold value. The conflict risk is significantly reduced for the larger conflict radius, but the maneuver rate increases significantly.

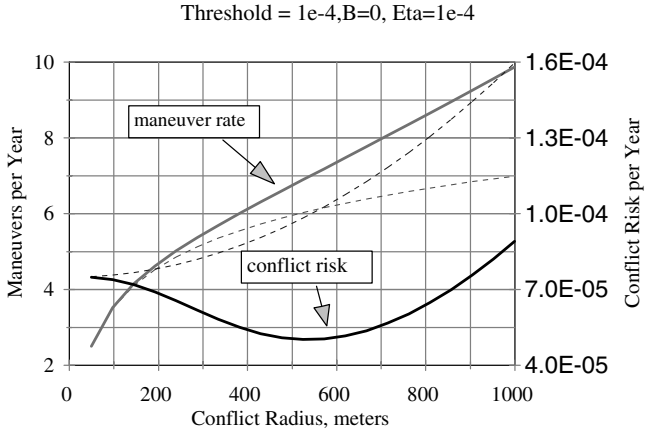

Fig. 10 Maneuver rate and conflict risk versus conflict radius.

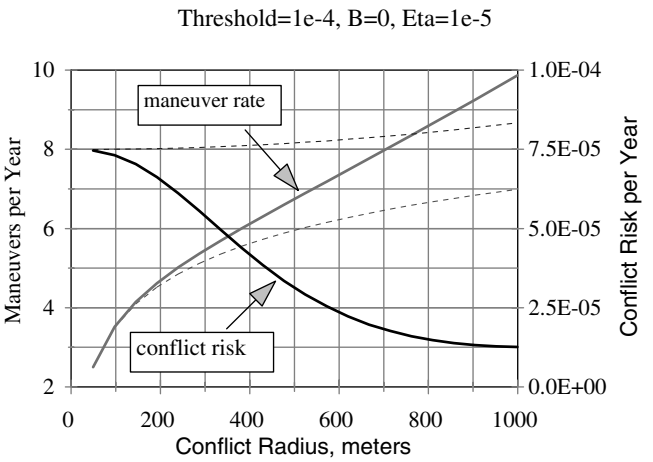

Fig. 11 Maneuver rate and conflict risk versus conflict radius.

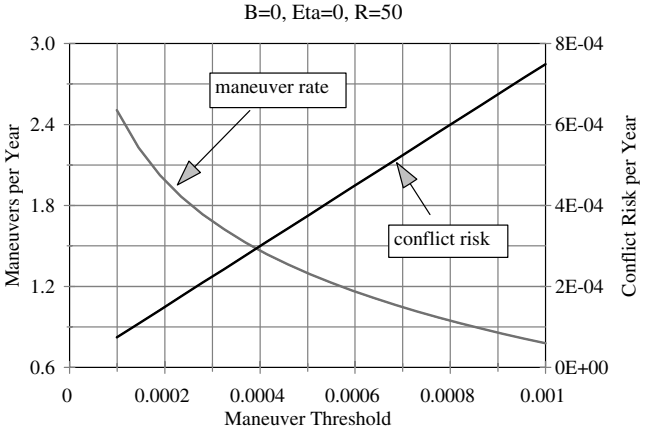

Fig. 12 Maneuver rate and conflict risk as a function of the maneuver threshold.

Figure 12 shows the dependence of the maneuver rate and conflict risk on the maneuver threshold for the same case as in Fig. 9, but with fixed R and variable threshold. Because the conflict volume radius is only 50 m, Eqs. (12) and (13) yield correct results. Therefore, both methods provide correct results and the heavy and dashed curves overlap. This case provides a measure of validation for Eqs. (12) and (13) and the current conflict risk analysis, which is valid for both small and large conflict volumes.

Figure 13 illustrates maneuver rate and conflict risk versus maneuver threshold for the case in Fig. 12, but with a conflict volume radius of 1 km instead of 50 m. In this case, Eqs. (12) and (13) yield

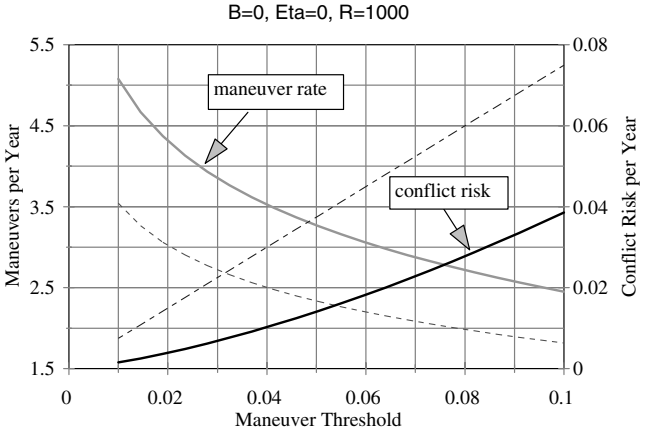

Fig. 13 Maneuver rate and conflict risk versus maneuver threshold for a 1-km conflict volume radius.

incorrect results, because the conflict size is not small with respect to the position-error uncertainty. The erroneous results are shown in Fig. 13 for comparison purposes. As the threshold increases, fewer maneuvers are performed and the less reduction in conflict probability is realized. The correct analysis requires greater maneuver rate, but provides greater reduction in conflict probability.

Conclusions

Conflict probability was adopted from the aviation industry as a metric for quantifying collision risk. Because a fixed conflict volume replaces combined space vehicle and debris object hardbody size, it eliminates uncertainties in hardbody size estimation used in collision probability calculations. In addition, conjunction statistics of three known space collision events indicate that conflict probability is a better indicator of collision risk than collision probability. Long-term collision risk reduction methods were successfully applied to conflict risk reduction. Use of conflict probability is beneficial to future programs, such as reusable launch vehicles, that require collision avoidance in both air and space environments.

Acknowledgments

Thanks are extended to Vladimir Chobotov, Charles Gray, and James Paget for reviewing this document and providing valuable suggestions. The author greatly appreciates the work of Eric George in developing the statistical conjunction data for actual space collision events.

References

[1] Berend, N., "Estimation of the Probability of Collision Between Two Catalogued Orbiting Objects," *Advances in Space Research*, Vol. 33, No. 1, 1999, pp. 243–247.

[2] Alfriend, K. T., Akella, M. R., Lee, D., Frisbee, J., and Foster, J. L., "Probability of Collision Error Analysis," *Space Debris*, Vol. 1, No. 1, 1999, pp. 21–35.

[3] Chan, K., "Collision Probability Analysis for Earth Orbiting Satellites," *Advances in the Astronautical Sciences*, Vol. 96, Univelt, San Diego, CA 1997, pp. 1033–1048.

[4] Patera, R. P., "General Method for Calculating Satellite Collision Probability," *Journal of Guidance, Control, and Dynamics*, Vol. 24, No. 4, 2001, pp. 716–722.

[5] Patera, R. P., "Method for Calculating Collision Probability Between a Satellite and a Space Tether," *Journal of Guidance, Control, and Dynamics*, Vol. 25, No. 5, 2002, pp. 940–945.

[6] Patera, R. P., and Peterson, G. E., "Space Vehicle Maneuver Method to Lower Collision Risk to an Acceptable Level," *Journal of Guidance, Control, and Dynamics*, Vol. 26, No. 2, 2003, pp. 233–237.

[7] Patera, R. P., "Satellite Collision Probability for Non-Linear Relative Motion," *Journal of Guidance, Control, and Dynamics*, Vol. 26, No. 5, 2003, pp. 728–733.

[8] Patera, R. P., "Collision Probability for Larger Bodies Having Non-Linear Relative Motion," *Journal of Guidance, Control, and Dynamics*, Vol. 29, No. 6, 2006, pp. 1468–1472; also American Astronautical Society Paper 05-309, Aug. 2005.

[9] Alby, F., Lansard, E., and Michal, T., "Collision of Cerise with Space Debris," *Proceedings of the Second European Conference on Space Debris*, ESA Publications Div. of European Space Research and Technology Centre, Noordwijk, South Holland, The Netherlands, 1997, pp. 589–596.

[10] Peterson, G. E., "Determining Object Sizes from Radar Cross Section for Collision Avoidance," Astrodynamics Specialists Conference, Lake Tahoe, CA, American Astronautical Society Paper 05-307, Aug. 2005.

[11] Paielli, R. A., and Erzberger, H., "Conflict Probability Estimation for Free Flight," *Journal of Guidance, Control, and Dynamics*, Vol. 20, No. 3, 1997, pp. 588–596.

[12] Committee on Space Shuttle Meteoroid/Debris Risk Management *Protecting the Space Shuttle from Meteoroids and Orbital Debris*, National Academy Press, Washington, D.C. 1997.

[13] Committee on Space Shuttle Meteoroid/Debris Risk Management, *Protecting the Space Station from Meteoroids and Orbital Debris*, National Academy Press, Washington, D.C., 1997.

[14] Gist, R. G., and Oltrogge, D. L., "Collision Vision: Covariance Modeling and Intersection Detection For Spacecraft Situational Awareness," Astrodynamics Specialist Conference, Girdwood, AK, American Astronautical Society Paper AAS-351, Aug. 1999.

[15] Foster, J. L. Jr., "The Analytical Basis for Debris Avoidance Operations for the International Space Station," *Third European Conference on Space Debris*, ESA Publications Div. of European Space Research and Technology Centre, Noordwijk, South Holland, The Netherlands, 1997, pp. 589–596.2001, pp. 441-445.

[16] Jenkin, A. B., "Effect of Orbit Data Quality on the Operational Cost of Collision Risk Management," SatMax 2002, Arlington, VA, AIAA Paper 2002-1810, Apr. 2002.

[17] Patera, R. P., "Parameter Relations in Orbital Collision Risk Reduction," 55th International Astronautical Congress, Vancouver, Canada, International Astronautical Congress, Paper IAC-04-IAA.5.12.5.06, Oct. 2004.

[18] Anon., "Accidental Collisions of Cataloged Satellites Identified," *Orbital Debris Quarterly News, NASA*, Vol. 9, No. 2, 2005, pp. 1–2.

[19] Alfano, S., "Relating Position Uncertainty to Maximum Conjunction Probability," *Journal of the Astronautical Sciences*, Vol. 53, No. 2, 2005, pp. 193–205.